Supplementary Material

Conductive PDA@HNT/rGO/PDMS aerogel composites with significantly enhanced durability and stretchability for wearable electronics

Hailong Hu[1], Yalun Ma[1], Yusuf Abdullahi Hassan[1], Lei Chen[2], Jing Ouyang[3,4], Huaming Yang[3,4], Fan Zhang[3,4]

[1]Research Institute of Aerospace Technology, Central South University, Changsha 410083, Hunan, China.
[2]Center of Materials Science and Optoelectronics Engineering, University of Chinese Academy of Sciences, Beijing 100049, China.
[3]School of Minerals Processing and Bioengineering, Central South University, Changsha 410083, Hunan, China.
[4]Hunan Key Laboratory of Mineral Materials and Application, Central South University, Changsha 410083, Hunan, China.

Correspondence to: Dr. Fan Zhang, School of Minerals Processing and Bioengineering, Central South University, No. 932, Yuelu District, Lushan South Road, Changsha 410083, Hunan, China; Hunan Key Laboratory of Mineral Materials and Application, Central South University, No. 932, Yuelu District, Lushan South Road, Changsha 410083, Hunan, China. E-mail: fan.zhang@csu.edu.cn

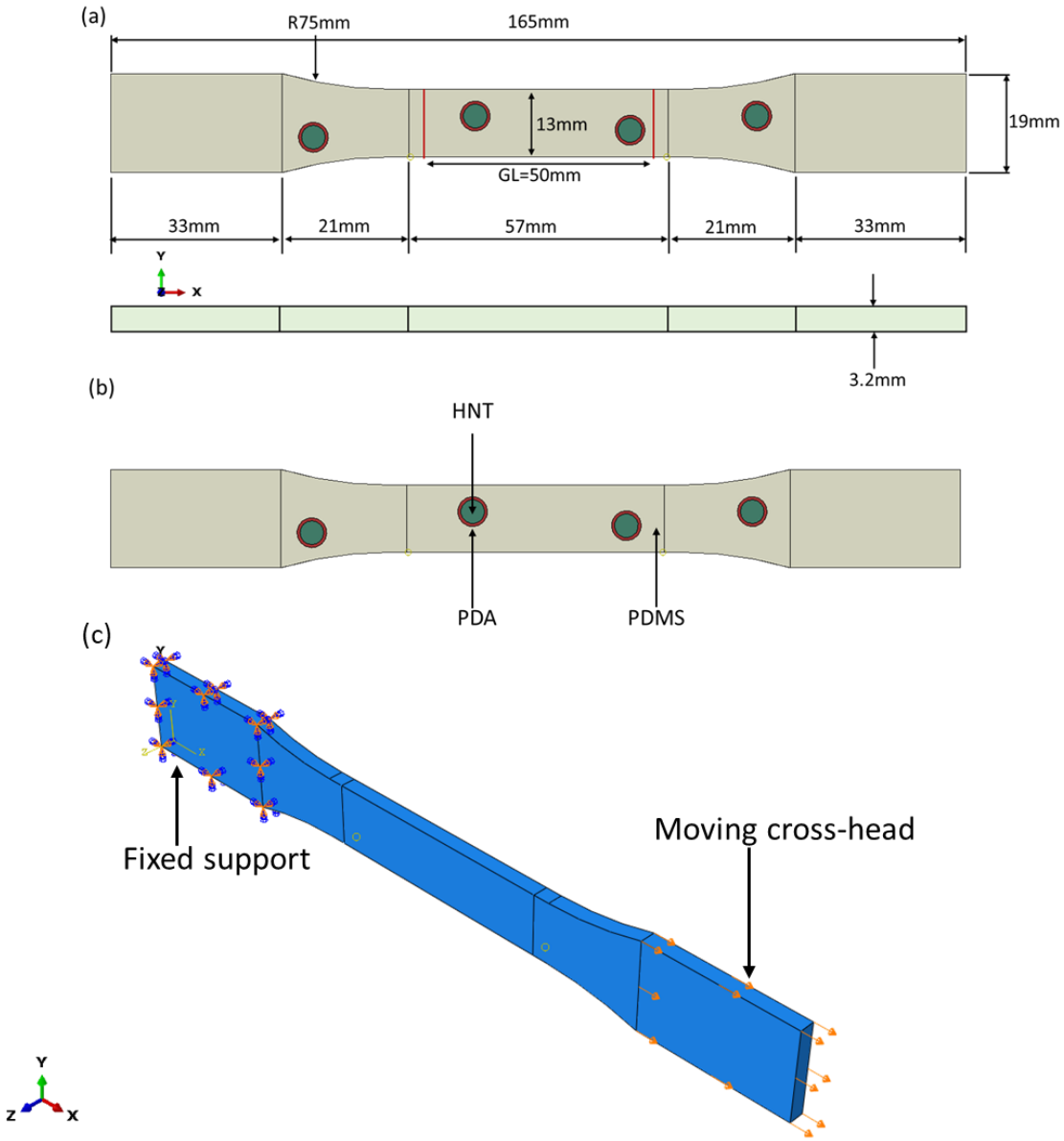

Fig. S1 a) The design parameter of the model, b) core-shell structural design, c) applied load.

The designed parameters of the model are shown in Fig. S1a. The original length of the samples used is 165 mm with a gauge length of 50 mm. As depicted in Fig. S1b, the core-shell structural design consists PDA coated HNT fillers (1:4). The base of the specimen is fixed using ENCASTRE boundary condition in ABAQUS i.e., U1=U2=U3=UR1=UR2=UR3=0. Additionally, a 5 N force is applied to the front head of the specimen during the analysis as shown in Fig. S1c.

Fig. S2 illustrates the core-shell structural design of the sensing material with varying contents of PDA@HNT utilized in the simulation analysis. The fibers within the PDMS matrix are evenly distributed using the linear pattern option in ABAQUS. However, the volume content of the fibers is regulated by adjusting the number of fibers in the PDMS matrix through the equation presented below (Eq. 1).

$$V_f = \frac{4N\pi D^3}{24LWH} \qquad (1)$$

Where N represents the number of fibers, L, W, and H depict the length, width, and height of the model respectively. To figure out the exact number of fibers to meet the required volume fraction inside the matrix, Equation 1 is modified into Equation 2.

$$N = \frac{24LWH}{4\pi D^3} \qquad (2)$$

The FEA calculation performed during the modelling is based on the above equations where $\varepsilon_N = \frac{\Delta L}{L_0}$, $\Delta L = \varepsilon_N L_0 = 0.1 * 50 = 5mm$, with a proposed boundary conditions of 50% strain.

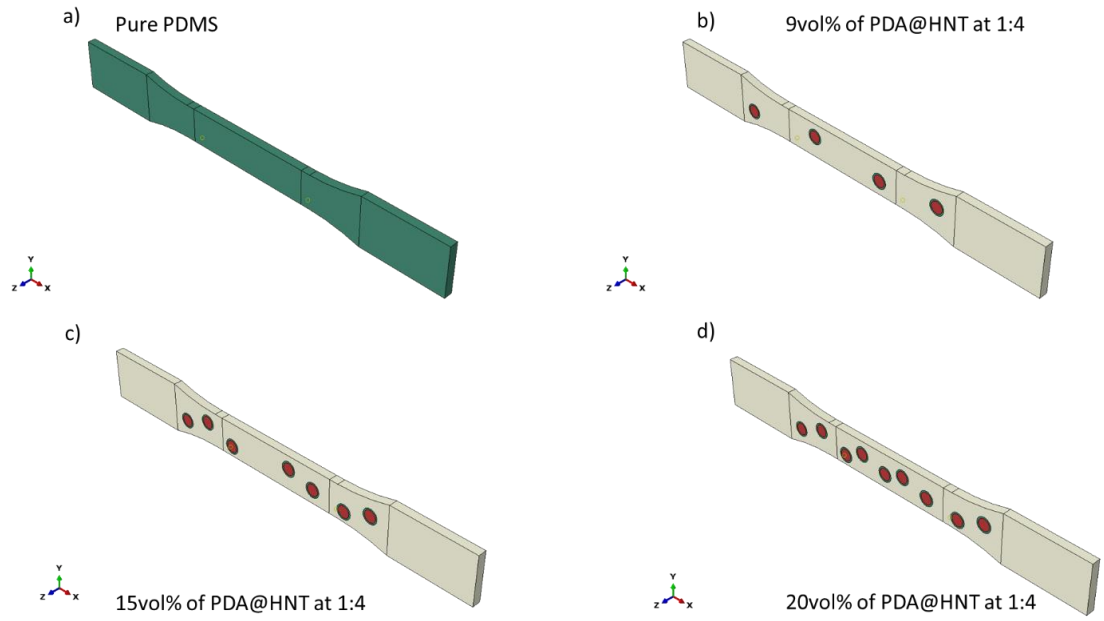

Fig. S2 Different contents of PDA@HNT fibers inside PDMS matrix.

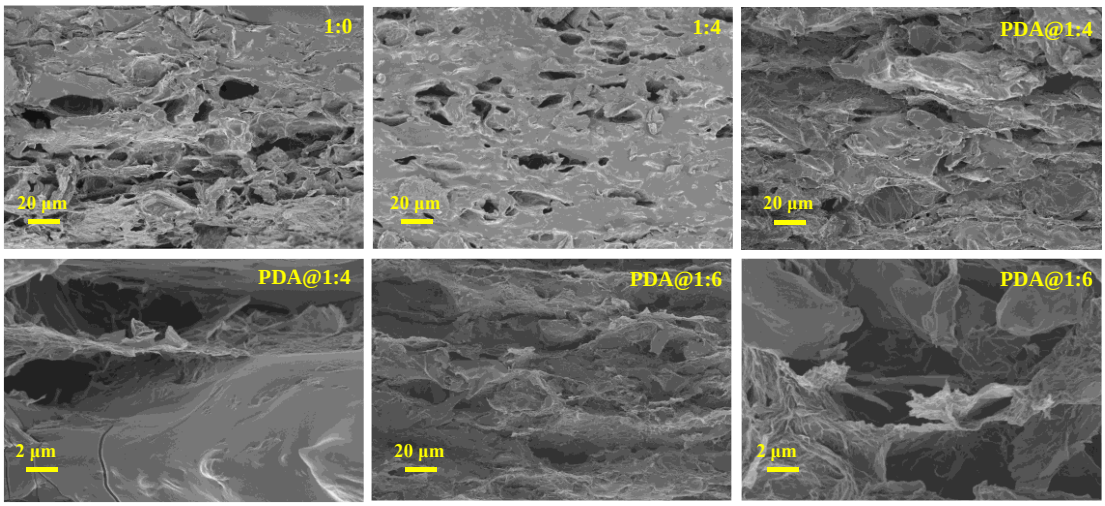

Fig. S3 Cross-sectional images of PDA@HNT/rGO/PDMS composites with different ratios of PDA@HNT to rGO: (a) without GO; (b) with HNT at a ratio of 1:4; with PDA being surface modified at a ratio of (c)-(d) 1:4 and (e)-(f) 1:6) at a GO concentration of 5.0 mg/ml.

The morphology of the conductive layer and its interaction with the polymer matrix significantly affect the conductivity and sensing behaviour of the core-shell strain sensor. To investigate this, we prepared PDA@HNT/rGO/PDMS composites with different weight ratios (HNT:GO=1:0, 1:1, 1:2, 1:4, 1:6, and 1:8) by controlling the weight ratio of HNT or PDA@HNT to GO. The cross-sectional SEM images presented in Fig. S3 show that the conductive fillers are unevenly dispersed into the polymer matrix due to their nanosize effect. In contrast, the sprayed PDA@HNT is evenly embedded in PDMS without any obvious aggregations, indicating that the nanofillers penetrate into the PDMS substrate rather than sticking to its surface. This contributes to improved stability and reproducibility of the detected operations and makes the fillers less brittle under extreme strain conditions, thereby increasing the sensing range of the composites.

The finite element calculations were carried out using COMSOL software. The mechanical performance of the model was analyzed using the solid mechanics module, and the electrical performance was analyzed using the current module. As shown in Fig. S4a, in the electrical analysis, a Voronoi diagram is first used to segment the equivalent resistive network of stacked graphene sheets. The overlapping regions between the graphene sheets, i.e., the intermediate layer, have a resistivity of 20 Ω·m, which is even eight orders of magnitude higher than that of the internal resistivity [1, 2]. Therefore, to simplify the analysis, the resistance within the graphene nanosheets themselves is not considered during the simulation process; only the resistance of the graphene nano intermediate layer is taken into account. Consequently, the equivalent resistive network at the boundary of a single-layer graphene nanosheet only considers the resistance of the overlapping region, which depends solely on its stacking degree in Fig. S4a. As illustrated in Fig. S4b, for the neighboring graphene nanosheets in this equivalent resistive network, when random values are assigned to the stacking degree a within the range of 0 to 1, an increase in GNP content tends to favor higher stacking degrees, making it more likely to randomly select a higher value. The regularized single-layer graphene nanosheet structure model is subjected to finite element calculations with random stacking degree values of Fig. S4a, employing a steady-state study approach. As the tensile strain increases, the stacking degree gradually decreases.

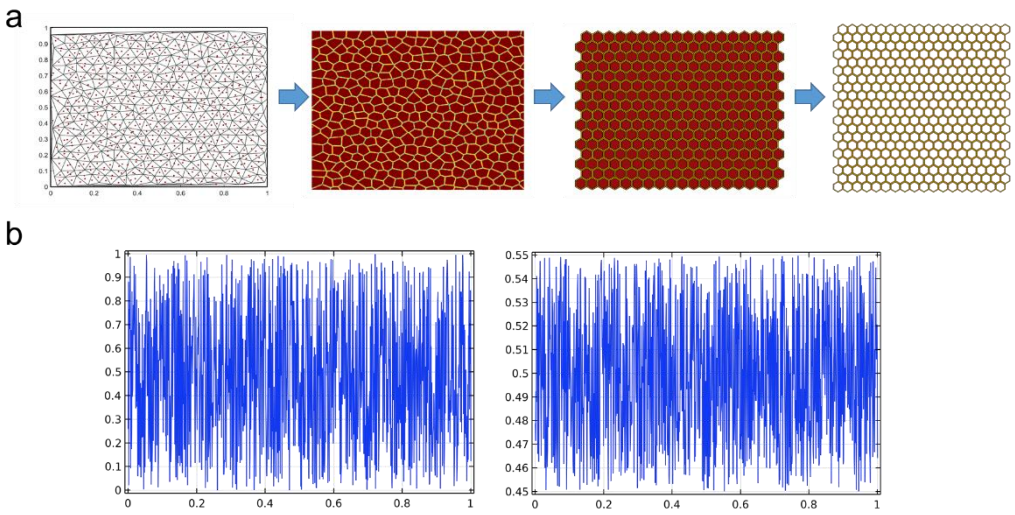

Fig. S4 FEA analysis

Table S1 Comparison of sensing performance between the developed composite strain sensor in this work and those of recently reported composite strain sensors.

Material type	Range of linearity	Sensing range	Cycles	References
GO/PDA@HNT/PDMS composites	**57.7%**	**73.2%**	**1000**	**This work**
Graphene-Polymer Composite Coatings	0.3%	0.5%	5	Adv Funct Mater 24 (2014) 2865–2874
GO/ PEDOT:PSS/PDMS composites	25%	45%	1000	Compos Sci Technol 187 (2020) 107959
SCFs/CNFs/PDMS composites	10%	15%	300	Compos Sci Technol 165 (2018) 131-139
GNP/PDMS composites	45.0%	69.7%	1000	Compos Commun 29 (2022) 101033
TiO_2@CF/PDMS composites	10%	55.2%	1000	J Adv Ceram 10 (2021) 1350–1359

CNF/GNP/PDMS composites	50%	60%	1000	Compos Sci Technol 172 (2019) 7-16

References

[1] Breakdown of the Interlayer Coherence in Twisted Bilayer Graphene[J]. Physical Review Letters, 2013, 110(9): 96602-96602.

[2] Nirmalraj P N, Lutz T, Kumar S, et al. Nanoscale mapping of electrical resistivity and connectivity in graphene strips and networks[J]. Nano Letters, 2011, 11(1): 16.